2016

Co-evaporated perovskite solar cells

Sabrina Stark
Iowa State University

Co-evaporated perovskite solar cells

by

Sabrina Stark

A thesis for master submitted to the graduate faculty

in partial fulfillment of the requirements for the degree of

MASTER OF SCIENCE

Major: Electrical Engineering

Program of Study Committee
Vikram Dalal, Major Professor
Rana Biswas
Ruth Shinar

Iowa State University

Ames, Iowa

2016

TABLE OF CONTENTS

ABSTRACT

Perovskite solar cells have become the dominant silicon alternate in the last few years. Within this thesis, thermal co-evaporation method is put forth as a potential method for producing high efficiency solar cells. Focus is given to producing higher efficiency cells primarily by monitoring and altering the contribution of the component materials of lead iodide and methylammonium iodide, as well as the overall thickness of the active layer, and the concentration of the poly[bis(4-phenyl)(2,4,6-trimethylphenyl)amine hole transport layer.

ACKNOWLEDGEMENTS

I would like to thank all those that helped me be able to succeed on a daily basis. First I would like to thank Vikram Dr. Vikram Dalal, for pushing me to always be better, and never allowing me to accept mediocrity. Next I would like to thank my committee members for sharing their time helping me get to this point.

Thank you to all of my colleagues at MRC who helped me in all the small and large ways to helped me succeed. I want to especially thank Ranjith Kottokkaran for always supporting me and giving me guidance on my project, Max Novak for not only creating and maintaining our system, but helping each us keep our spirits up and systems running. I would also like to thank all those that helped with measurements and process. Without Istiaque Hossain, Behrang Bagheri, Harshavardhan Gaonkar, and Mahendra Singh Dhaka to help me actually get through all the devices I would have never been able to sleep. I would not been able to get to this point without the mentorship along the way by Mehran Samiee Esfahani, Shantan Kajjam, Siva Konduri, Joydeep Bhattachaya, Hisham Abdussamad-Abbas, Pranav Joshi, and Brian Modtland. Thanks for each of you taking the time to show me the ropes, and never saying that you were too busy.

I would like to give thanks to my family and close friends, those that stood by me when my nerves were running thin, and my stress levels high. Thanks to my wife Sara Stark, for always caring and making sure I wasn't going to give up. Lastly i want to thank my parents Erin and Rich Goodson, for believing in me and

forcing me to take breaks and see them often enough that I didn't go crazy. It has been a long journey, but in the end it was all worth it

CHAPTER ONE: INTRODUCTION

Our sun, Sol, is the true energy source for our planet. Even before the inception of solar cells, all energy came from it. Coal, geothermal, wind, natural gas, oil; all these sources of energy can be traced back to the sun's warmth and light. Solar cells are, in effect, just taking a more direct route to gain this energy. It is true that they are not as, and will likely never be as efficient as trees or other flora, but still they can help replace less renewable energy sources.

Solar Cells

Solar cells are one of a few simple semiconductor devices. In the simplest sense, they take in light and excite electrons to be collected to generate electricity. In this section we will go further into detail about how solar cells work. When exposed to light some semiconductors will produce a small current due to the photons energy being transferred to electrons in their lattice, this effect can be used to generate power known as solar energy. [4] Standard semiconductor photovoltaic cells use the absorbed photons to create electron hole pairs (EHP). This is done by exciting an electron from the valance band to the conduction band, creating excess charge carriers.[4] When this occurs in a p-n junction, the internal voltage will cause movement of the charged particles inducing a current in the material. By sandwiching two photoactive materials between metallic electrodes (one of which is transparent, and the other able to effectively absorb light) we are able to effectively collect photo generated charges.[4] The charges

move through the electrodes and produce current in the load by movement of holes and electrons. The junction depth must be small (less than the diffusion length of the holes in the n-type material) to allow holes generated at the surface to diffuse to the junction and recombine. Similarly, the thickness of the p-type layer must be thin enough to allow electrons to easily diffuse through to the junction before recombination occurs. This requires a proper match between the electron diffusion length and the thickness of the p-type region and the optical penetration depth of (1/a).

To obtain a large photovoltage, longer carrier lifetime, and low resistance, we have to maintain several parameters: namely a higher Vo and higher doping. This presents a problem as doping reduces lifetimes, but will likely increase the photovoltage. This leaves designers with a balance of properties that they can achieve and properties they desire. We want to keep resistance low so power lost due to heat is reduced. In the bulk material this is not hard, but within the thin top layer near the contact it isn't as simple. Near the contact the current must flow along the thin region to the contact, resulting in a large series resistance. To reduce this effect, contacts can be distributed over the top surface by having small contact leads all over the lighted surface. The distributed contacts serve to reduce the resistance without overly interfering with the incoming light.

Advancements in Perovskites

In 2012 the first perovskite solar cell with an efficiency exceeding 9% was made by Professor Snaith's group making use of a mesoporous Titanium oxide scaffold structure for the perovskite material to attach to. [2] This organic-

inorganic hybrid of sorts sent shockwaves through the solar cell research community. Many if not all groups then working on various types of organic solar cell research switched over to perovskite research due to its quick rise to high efficiencies. Below you can see a graph using data taken from NREL solar cell efficiency tables. It demonstrates that over the past few years the rise in efficiency of the perovskite solar cell over competing technologies.

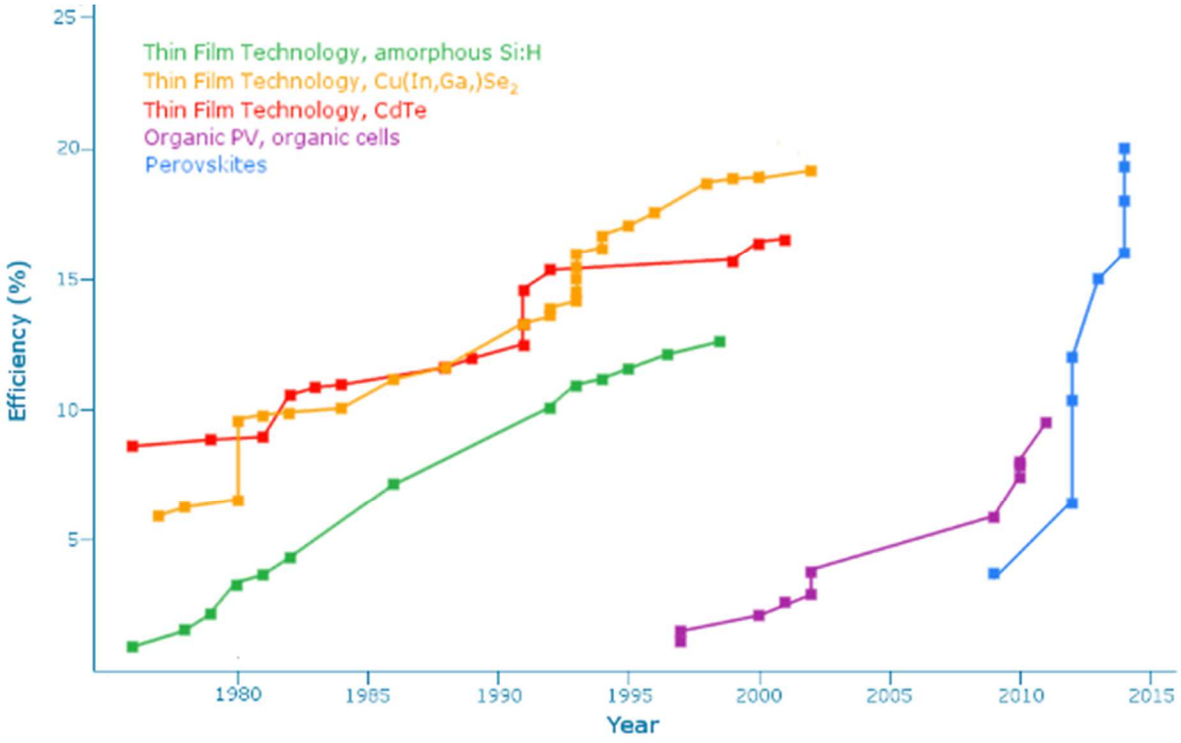

Figure 1: Efficiency curves of solar cell technologies by year.

The technology has gone from under 10% to over 20% in a span of 5 years. It's plain to see why people are scrambling to put effort into researching this technology. A perovskite, or rather the perovskite structure, is a combination of calcium titanium and oxygen, and was originally named after Lev Perovski, a Russian geologist that found the material in the Ural Mountains. For solar cell

researchers, anything with the generic ABX3 crystal structure is considered a "perovskite". In Fig 02 below you can see the ABX structure:

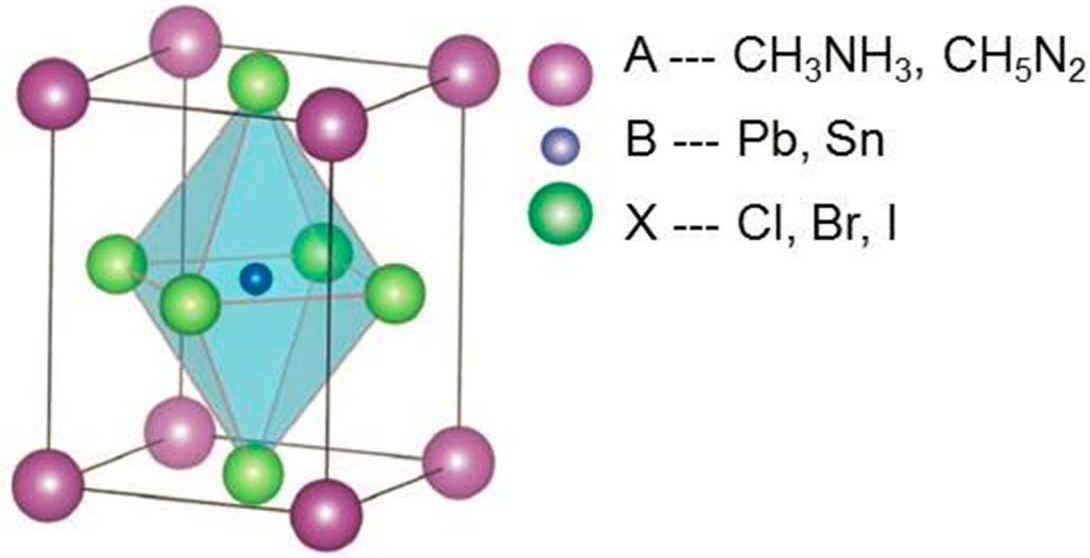

Figure 2: Perovskite molecular structure diagram

To form this ABX3 perovskite structure it needs to have a large positively charged molecular cation to form the outer "cube" of the structure made up of either methylammonium or imino methanaminium. Next we need several smaller negatively charged anions to form the internal "diamond" structure, made of either lead or tin. Then finally a smaller positively charged cation at the center made of chlorine, bromine or iodine. It has been found that by playing with the combinations of different A, B and X materials that we can get an array of properties out of the perovskite structure. These include large magnetoresistance, spin dependent transport, and even superconductivity. In the case of solar cell technology we have seen that the highest efficiencies have

been found in the combination of methylammonium, lead, and either chlorine or iodine.[3]

CHAPTER 2: FABRICATION

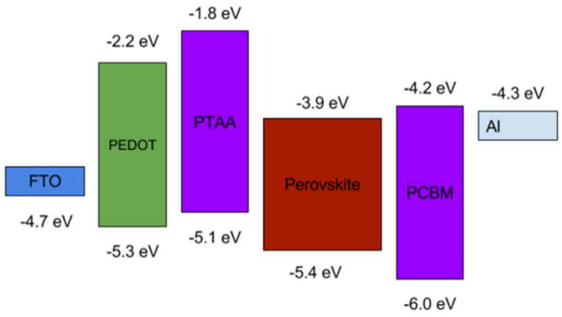

Figure 3: Energy Band Diagram

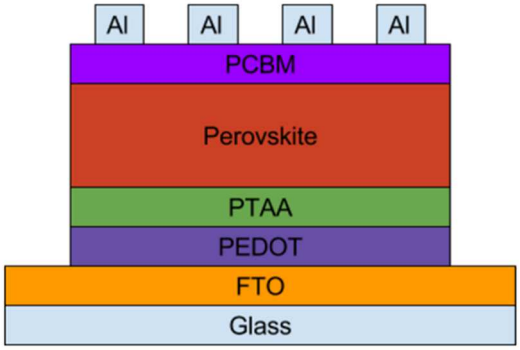

Figure 4: Cross Sectional Diagram

Introduction

Our solar cell production process can be broken up into several distinct modules. The first of these modules involves cleaning and preparing our substrates for deposition. The second being the steps needed to create our hole transport layers. The third is the creation of our active layer for the absorption of light. The last two modules are the deposition of the electron transport layer and the final top contacts.

Cleaning Steps

All samples in this study were deposited on glass slides coated with fluorine doped tin oxide. Each were cleaned using our standard cleaning methods. This is done by first sonicating in a surfactant bath, then thoroughly rinsing the slides. After that is complete we place them in a warm sonication bath

of acetone. Lastly we sonicate in methanol. We have found that this process has been sufficient for allowing us to have clean substrates to begin with. These cleaned substrates are then stored in new methanol before being used for deposition. Before we are able to deposit our hole transport layer on these substrates we must first do a plasma cleaning to remove any organic material. This step is done right before the next module is started.

Hole Transport Layers

Before we are able to move to thermal evaporation, we put on our hole transport layer of poly(3,4-ethylenedioxythiophene) polystyrene sulfonate (PEDOT:PSS) and Poly[bis(4-phenyl)(2,4,6-trimethylphenyl)amine] (PTAA). PEDOT:PSS was spin coated at 4000 rpm/40 sec and annealed 150°C for 20 min in air. PTAA layer was spin coated inside the glovebox at 6000 rpm/40 sec and annealed 150C/10 min. Afterward these are stored in a drybox to prevent the accumulation of moisture.

Co-Evaporation

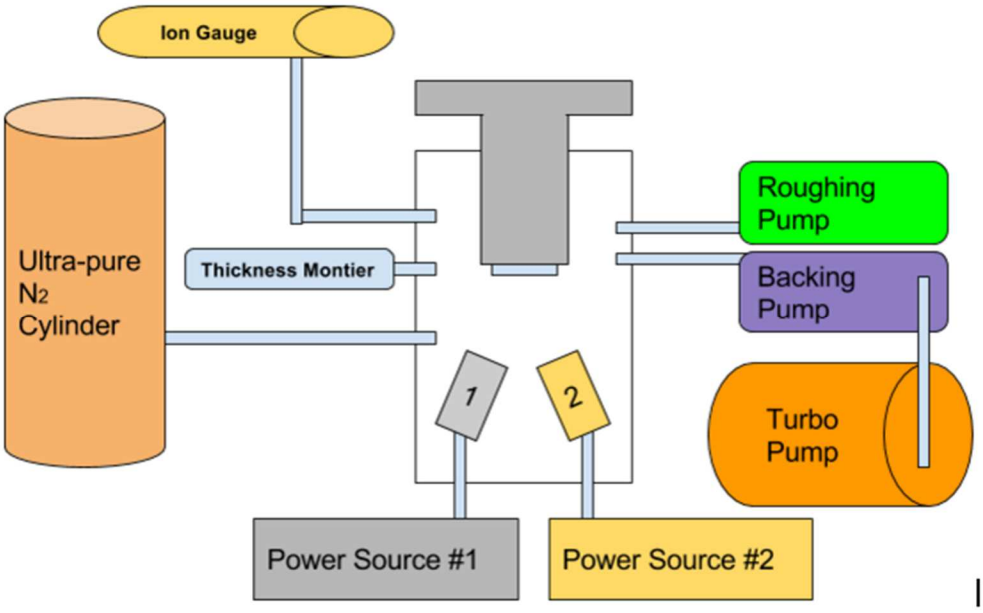

Figure 5: Coevaporation Thermal evaporation chamber "E4" diagram

After we have deposited PEDOT and PTAA on our substrates, we move to the co-evaporation stage of production. This is the most crucial state of production due to the multitude of variables that thermal evaporation entails. The thermal evaporation chamber we use has six basic systems that we use to control the system and monitor what is going on inside. The first and second are a set of two pumps: one for roughing and one for backing. To control these we have a switch to turn on the roughing pump and a gate valve to open up the chamber to our turbo pump. The third and fourth systems involve a series of two crucibles with heating coils surrounding them to heat up the necessary materials for deposition. These coils are controlled by two power supplies outside the

system. The fifth system is a pressure gauge which will give us the pressure of the system at any given time inside the chamber. The sixth system is a crystal thickness monitor that gauges how much material has been deposited on our substrate. In figure 06 below you can see the chamber we used to produce all the cells in this study.

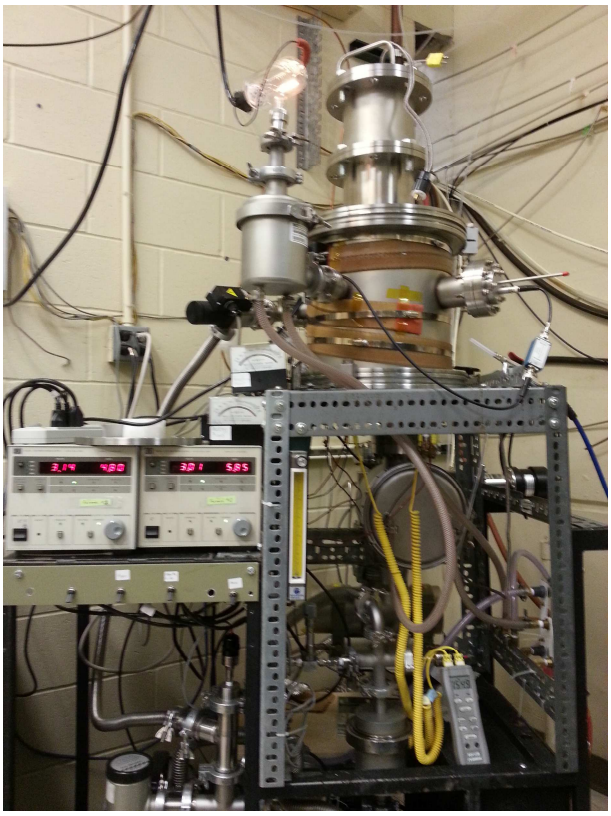

Figure 6: Co-evaporation Thermal evaporation chamber "E4" photo

Before we place the substrates into our chamber first we first heat them for 5 minutes at 100°C to drive out excess moisture that may remain on the substrates. Next we attach the substrate to our heater which also doubles as the upper plate of the vacuum chamber. For this experiment we did not make use of the substrate heater. Once the substrate is now secured to the substrate heated

and reattached to the chamber, we are able to do a purging process to remove any excess moisture and oxygen from the chamber. Once we have attained the pressure we require for the experiment we are then able to turn on the heater for the lead iodide crucible. We first make a layer of lead iodide this layer is approximately 5 nm thick and allows us to have some way of blocking the MAI from attaching directly to the substrate itself. Once the first layer is complete we close the shutter for the lead iodide and then also turn on the heater for the MAI. Once both are at the temperature we want then we are able to consider when we open the shutter for the lead iodide as the “start” of the run. We let the two materials react and form perovskite on our substrate. Once we have deposited the requisite amount the heaters are turned off and the chamber is allowed to cool down, and pump out excess MAI and lead iodide. After cooling down another purging process is completed to help prevent the materials from passing into the room’s atmosphere. Then we are able to remove the sample and place it into a nitrogen filled container for transport into our controlled nitrogen atmosphere glovebox for further development.

Electron Transport

Once the substrates are moved into the glovebox post annealing of the perovskite is carried out for 100 °C/ 1hr. This post annealing allows the complete formation of the perovskite. . Once that is completed we move to adding the electron transport layer of PCBM. This like the hole transport layers were deposited via spin coating only we spin coat inside the dry nitrogen atmosphere

of the glovebox instead of outside. The substrates are then annealed at 100 C/15 min

Contact Process

The final module of the process is to add the top contacts to our cells. This is done using a vacuum evaporation chamber inside the glovebox. The cells are masked so that six contacts of 0.106 cm2 are made. This allows us to have multiple individual solar cells on one substrate and we can then more easily have consistent data. A 100 nm of Aluminum was evaporated under 1E-6 Torr pressure. Once complete we are able to move to the characterization stage.

CHAPTER 3: CHARACTERIZATION

Once all the production processes have been completed we can move to measurement. Due to the hydrophilic nature of MAI and how the organic transport layers used in these cells, all the tests must be completed in a dry nitrogen atmosphere of a glovebox. The glovebox used for all measurements is one separated from the production glovebox to prevent any contamination from errant solvents.

Photocurrent Measurement

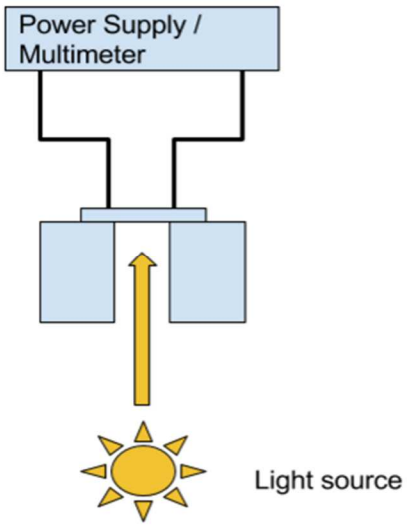

Figure 7: IV characterization station diagram

Figure 8: IV characterization station photo

Our first and most revealing measurement is current vs voltage (IV). In our standard characterization we set the voltage to be positive and the current to

negative from anode to cathode. From this measurement we can determine efficiency, fill factor, and the shape of the curve given can give us an idea of that is going on in the cell. The efficiency of the cell or rather the power conversion efficiency of the cell is the percentage of how much power is generated from the incident power of the light shown on the surface of the cell. Mathematically the efficiency of a cell is determined by the fill factor, open circuit voltage, and the short circuit current. The exact equation for efficiency can be found below;

$$\boldsymbol{E}(\%) = \frac{\boldsymbol{P_{out}}}{\boldsymbol{Pin}} = \frac{\boldsymbol{V_{oc}J_{sc}FF}}{\boldsymbol{P_{In}}}$$

Equation 1: Solar cell efficiency equation

At first glance it seems like as long as we make the open circuit voltage, short circuit current, and fill factor as high as we can we will get a higher overall efficiency, but our voltage is highly dependent on the bandgap. Effectively the bandgap will have to be “tuned” to what level of photons we want and generally the larger the band gap we have the smaller overall current density we will get out of the cell.

On the other hand fill factor is described as the ability for the cell to extract current at any given voltage. Mathematically it is the ratio of the maximum power output and the product of the short circuit current combined with the open circuit voltage. The equation for fill factor can be seen below.

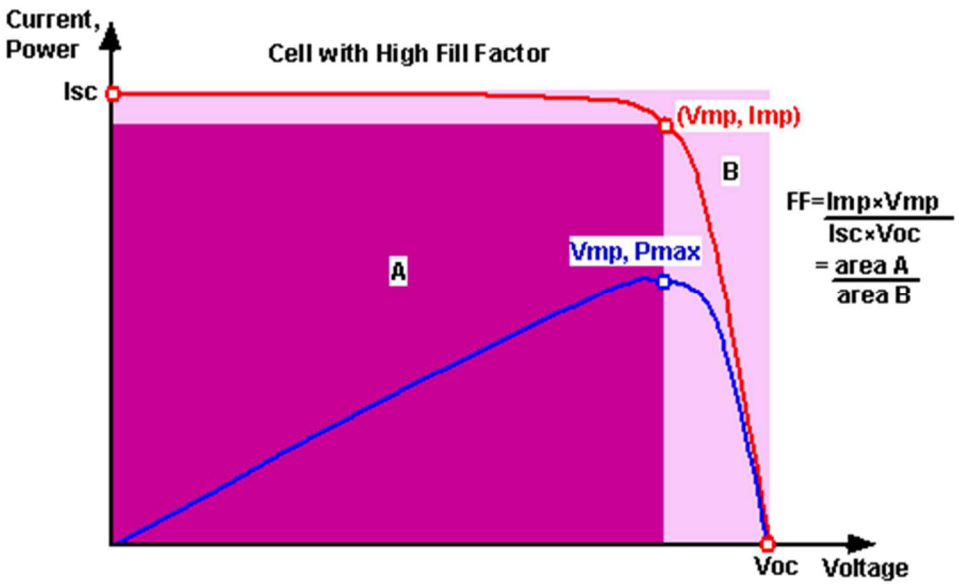

Figure 9: Solar cell fill factor diagram with IV curves

$$FF = \frac{P_{max}}{V_{OC} I_{SC}} = \frac{V_{MP} I_{MP}}{V_{OC} I_{SC}}$$

Equation 2: Fill factor equation

Shapewise, we know that the “squareness” of our curve can tell us many things. First, in general such “squareness” means that more current is being extracted. If we see more than one saturation level we may have either an interface an ohmic contact issue. It is also possible that the structure is malformed somewhere. If the right hand side of the curve is more of a ramp than a quick drop off we could have some sort of shunt problem. All of these issues tend to give you clues to what needs to be done to your cell to bring it closer to the ideal shape.

The IV characterization set-up used for all devices presented in this paper can be seen in figures 07 and 08. Due to the fact that our devices are not stable

in normal atmospheric conditions we have our system is a controlled dry nitrogen glovebox. Our systems consists of two probes one to connect to the cathode of our device and the other for the anode, and a ELH lamp that is roughly equivalent to one sun of optical input power. We use an automated system consisting of a labview program controlling a Keithley 236 source measure unit. The labview program first measures open circuit voltage and short circuit current and then moves on to do a 125 point sweep from -0.2 V-1V. Then the program calculates fill factor and efficiency for us.

Quantum Efficiency (QE) Measurements

Quantum efficiency (QE) experiments are used to explain the behavior of a solar cell at different wavelengths along the solar spectrum. First let's break down quantum efficiency into two separate parts. These separate parts are; external quantum efficiency (EQE), and internal quantum efficiency (IQE). EQE is the total number of carriers collected divided by the number of incident photons at a given area, at a given time. [4] To see this in a formulaic form please see Equation 03 below.

$$EQE = \frac{Electrons\ out}{Photons\ in} = \frac{Current/electron\ charge}{Total\ power/photon\ energy}$$

Equation 3: External quantum efficiency equation [4]

$$IQE = \frac{Electrons\ out}{Photons\ absorbed} = \frac{EQE}{1 - reflection - transmission}$$

Equation 4: Internal quantum efficiency equation [4]

IQE is the number of total number of carriers collected divided by the total number of photons absorbed, the equation for this can be seen in equation 03 above [4] One example of a typical EQE curve of a solar cell shown in figure 10

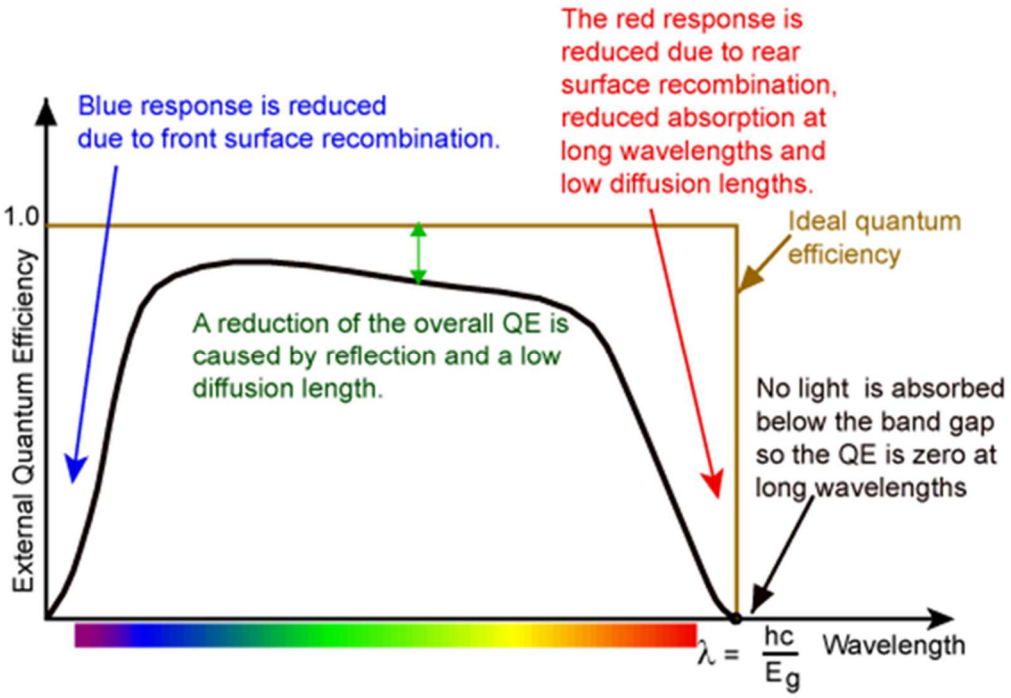

Figure 10: EQE vs Wavelength graph [5]

When different wavelengths of light are incident on a solar cell, the shorter wavelengths with higher absorption coefficient will quickly be absorbed within the first few hundred nms [4]. In contrast, the longer wavelengths will penetrate deeper and generate carriers all throughout the intrinsic layer.[4] This property helps us understand problems inherent with the interface and bulk absorption problems. For our cells the measurement was done at zero bias and at a negative bias of -1 V. Putting our cell under a negative bias will improve the electric field, which in turn will increase the overall collection of carriers. If QE

ratio is higher at shorter wavelengths, ie 400-500nm, then it is likely pointing to an interface problem somewhere between the i and p-layers. On the other hand if our QE ratio is higher at longer wavelengths, in the 800- 900nm range, then it may be a likely indication of a poor internal material property throughout the I layer in an p-i-n cell.

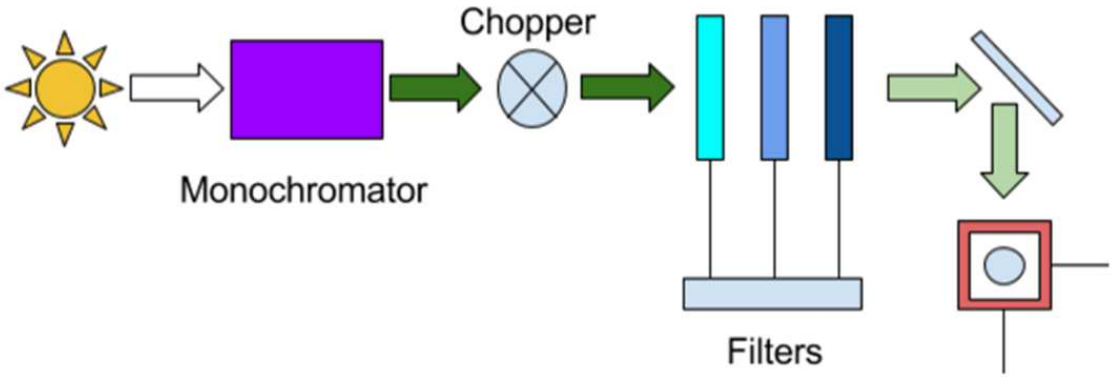

Figure 11: Quantum efficiency system schematic diagram

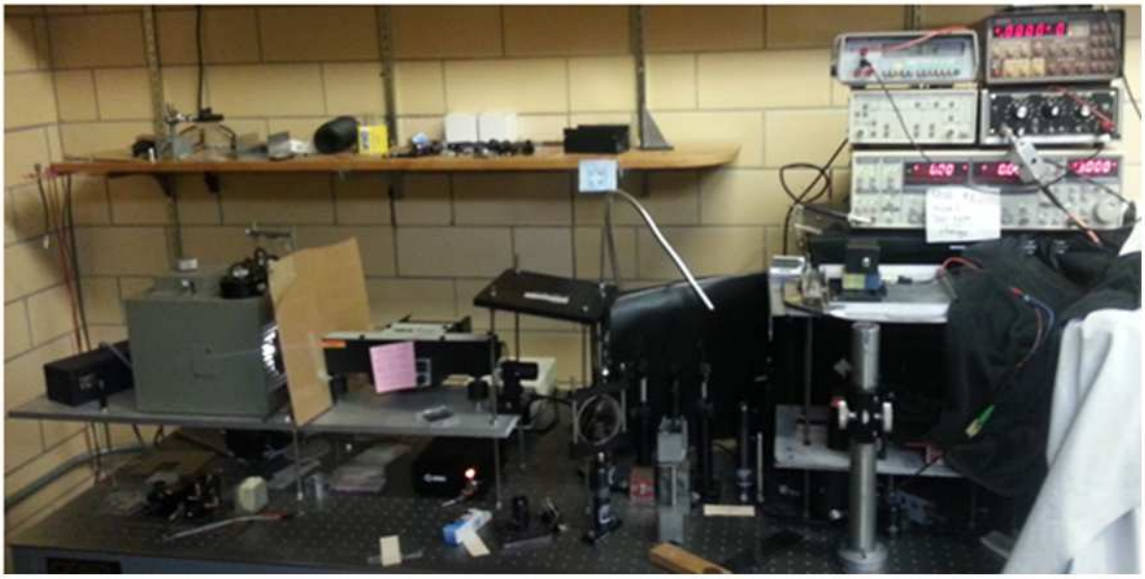

Figure 12: Quantum efficiency system picture

Figure 11 above shows both the schematic diagram and figure 12 a picture of the actual system used for the tests. All the discrete systems that make up the QE setup can be seen in the upper half of the figure the QE setup clearly showing all of the parts. This system consists of monochromator which makes use of a grating structure to cut out all wavelengths of light that we do not want to only output light of particular wavelength. Next the light from the monochromatic source passes through a rotating chopper moving at a frequency of 13.56 Hz. So that the the system can make use of this AC light to try and filter out all other ambient light, by making use of a lock-in amplifier, programmed to lock onto the frequency of the chopper. Then the light is focused using a series of lenses. Lastly, a mirror is used to reflect the light onto either the cell or the reference photodiode. The reference photodiode we use is a standard silicon photodiode whose QE response is known and referenced. The cells are also soaked in DC light to help fill the midgap states with photogenerated carriers, and pin our quasi fermi levels. Filters are used at 580nm, 700nm and 900nm to reduce noise from the lower harmonics. The wavelength emitted by the monochromator is varied and the signal is recorded.

CHAPTER 4: DATA AND RESULTS

In this section we will go over the data collected from a series of runs completed for the purpose of achieving higher efficiency cells using the co-evaporation method of producing perovskite solar cells. For this data set we will be focusing on controlling the MAI pressure in the chamber, the PTAA solution concentration, and post-deposition annealing conditions. These conditions were found to be the most important in controlling the lead iodide to MAI ratio necessary for producing higher efficiency perovskite solar cells.

The first experiments ran involved seeing if we would get better cells if we annealed both with and without the presence of MAI. The annealing step was performed inside of a glovebox with a nitrogen atmosphere with monitored oxygen and moisture levels in the <2 ppm. Each Sample was heated on a hotplate inside of a sealed graphite dish. Each of these cells had a PTAA concentration of 4.2mg/mL and were co-evaporated for 75 mins, with an MAI pressure of 7E-5 to 8E-5. The lead iodide temperature was between 315 and 320 degrees celsius. In figure 13 below you can see the results of this part of the study.

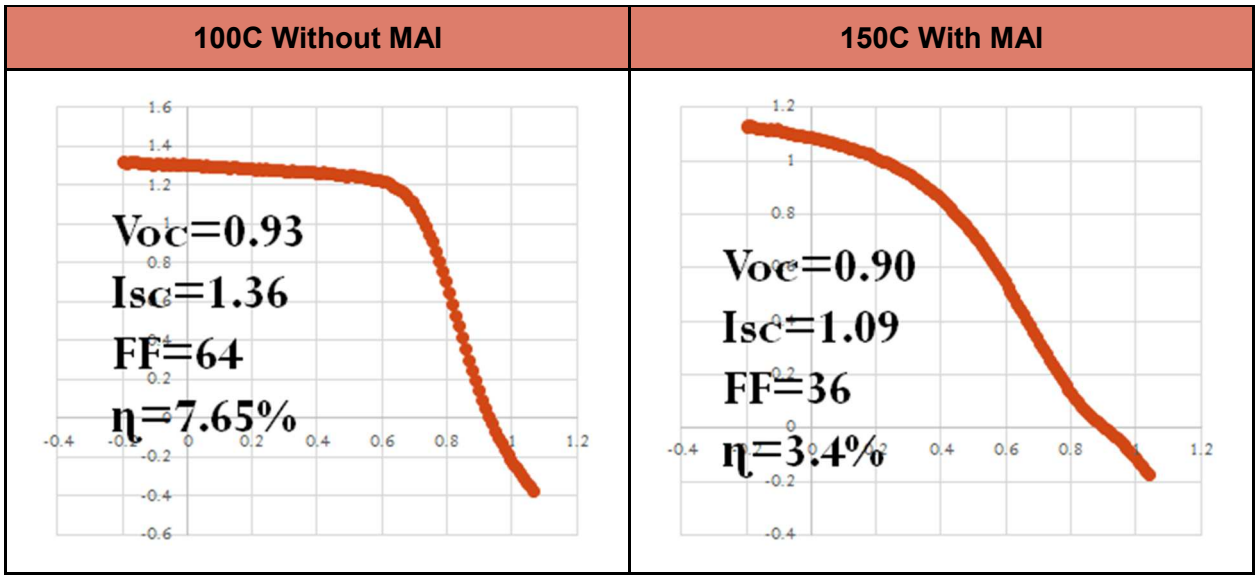

Figure 13: IV data comparing cells made with and without MAI post processing

As you can see we had over double the efficiency without using MAI in our annealing process. This is likely due to the fact that we have more MAI in our cells during the co-evaporation process as a percentage as a whole or possible due to the fact that the perovskite structure we have formed is more stable at 100 C than the solution based cells.

We have double diode in the device. Ie, there is an ohmic contact issue. In order to solve that we have reduced the thickness of PTAA by decreasing the concentration from 4.2 to 2.1 mg/mL

Next we moved on to changing the pressure of MAI in the chamber. We quickly found that in our runs it was important to control the MAI pressure to allow for us to have a consistent amount of MAI in the chamber at anytime to correspond to our amount of PbI2 which was much easier to control how much was being deposited at any one time. Any excess of the MAI or PbI2 would allow

for blocking layers to form in the perovskite layer. Below in figure 14 (pg 20-21) and table 01 you can see that we kept the PTAA concentration, the annealing time and temperature, the PbI2 temperature and the deposition time all constant and only varied the MAI pressure.

Mai Pressure of 5 to 7.5 E-5 Torr	Mai Pressure of 7.5 to 8.5 E-5 Torr
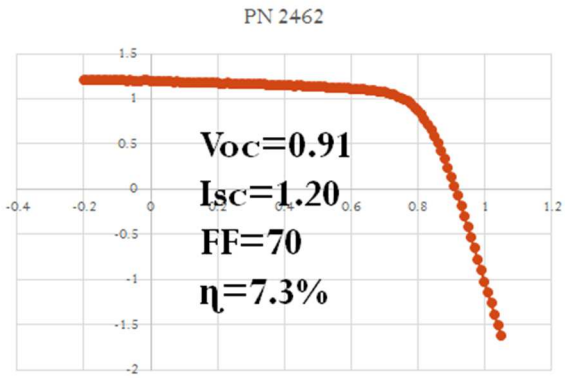	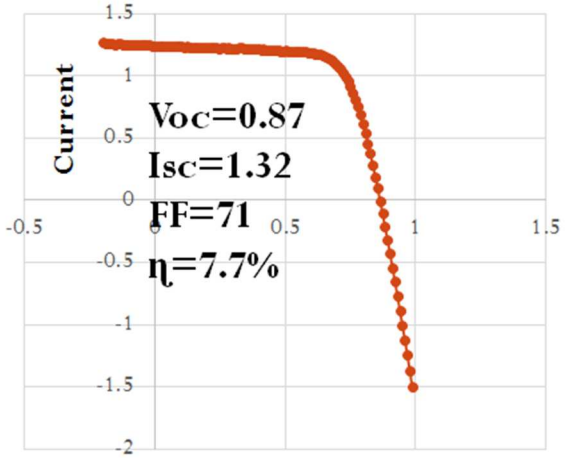
MAI Pressure of 9-10E-5 Torr	**Mai Pressure of 10 to 15 E-5 Torr**
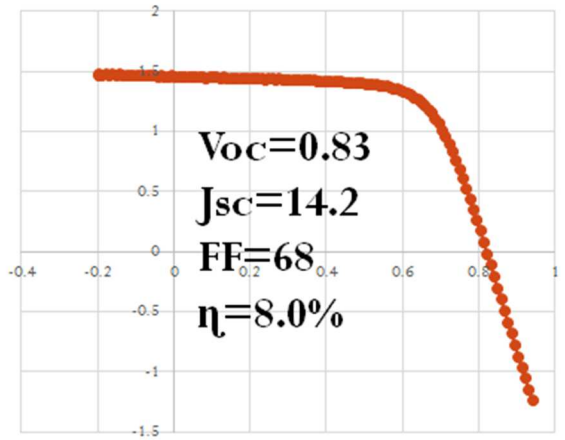	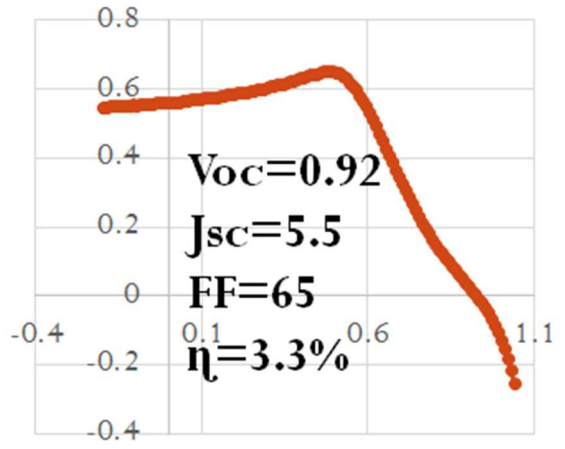

Figure 14: IV data comparing cells with different levels of MAI pressure

Table 1: Comparison of conditions used with variation of MAI Pressure

Time	PTAA Concentration	Annealing	PbI2 Temp	MAI Pressure	Efficiency
75 mins	2.1 mg/mL	100C/1 hour	315-320 C	5-7.5 E-5 Torr	7.30%
75 mins	2.1 mg/mL	100C/1 hour	315-320 C	7-8 E-5 Torr	7.70%
75 mins	2.1 mg/mL	100C/1 hour	315-320 C	9-10 E-5 Torr	8.00%
75 mins	2.1 mg/mL	100C/1 hour	315-320 C	10-15 E-5 Torr	3.3%

You can see that we found that 9-10E-5 T was our best case for the MAI pressure, for the PbI2 temperature of 315 to 320C. We used this pressure of MAI moving forward into our experiments with varying the concentration of PTAA.

The next experiment involved changing the overall concentration of PTAA. We left the deposition time, annealing conditions, PbI2 temperature, and MAI pressure all constant and only varied the PTAA concentration.We found that if we lowered the concentration of PTAA that we were able to increase the efficiency of our solar cells. This data can be seen below in figure 15 and table 02.

PTAA Solution of 1.45 mg/mL	PTAA Solution of 2.1 mg/mL	PTAA Solution of 4.2 mg/mL
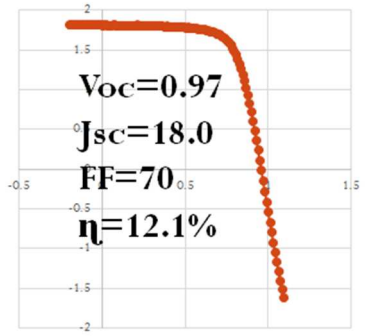	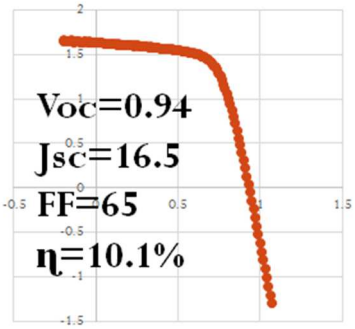	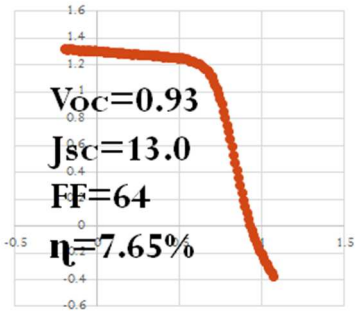

Figure 15: IV data comparing cells with different concentrations of PTAA solution.

Table 2: Comparison of conditions used with variation of PTAA solution concentration

Time	PTAA Concentration	Annealing	PbI2 Temp	MAI Pressure	Efficiency
75 mins	4.2 mg/mL	100C/1 hour	315-320 C	9-10 E-5 Torr	7.65%
75 mins	2.1 mg/mL	100C/1 hour	315-320 C	9-10 E-5 Torr	10.1%
75 mins	1.45 mg/mL	100C/1 hour	315-320 C	9-10 E-5 Torr	12.1%

Lastly we worked on changing the overall thickness of our co-evaporated layer. This involved changing the deposition time inside the chamber. First we explored using 75 mins, 80 mins and 90mins. This data is shown in figure 16 and 17 and table 03 We found that there was no significant difference between these three so we moved to 60 mins

75 mins	80 mins	90 mins
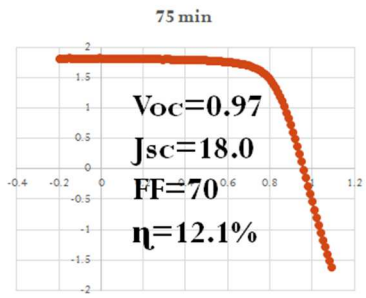	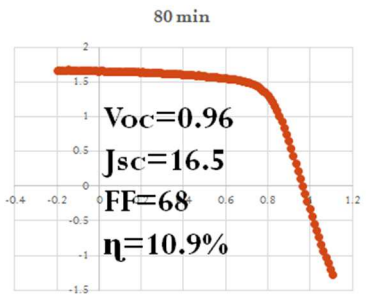	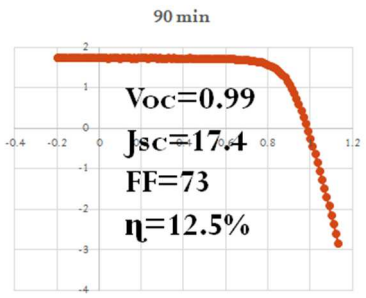

Figure 16:IV data comparing cells with different deposition times

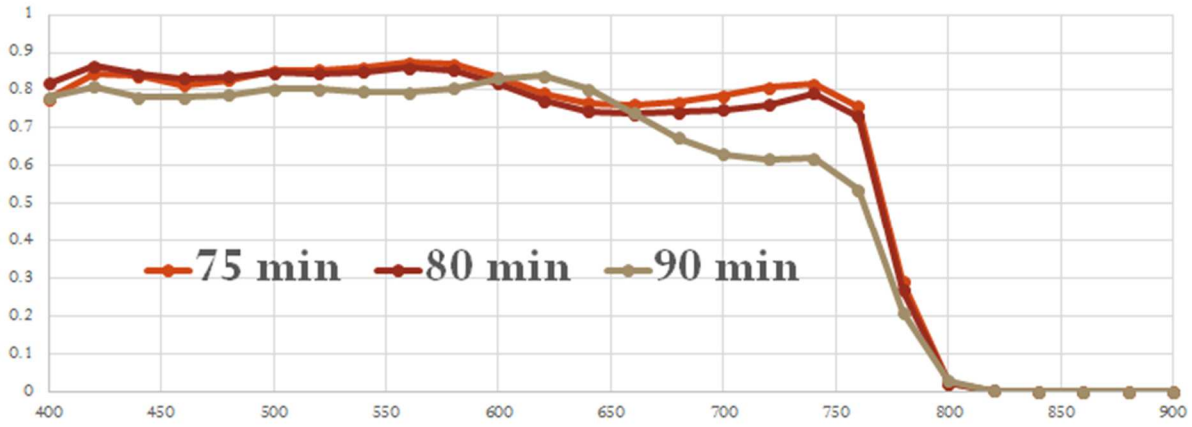

Figure 17: QE data comparing cells with different deposition times

Table 3: Comparison of conditions used with variation of deposition time

Time	Thickness	PTAA Conc.	Annealing	PbI2 Temp	MAI Pressure	Efficiency	QE (Jsc)
60 mins	280-290 nm	1.45 mg/mL	100C/1 hour	315-320 C	9-10 E-5 Torr	15%	19.02
75 mins	300-320 nm	1.45 mg/mL	100C/1 hour	315-320 C	9-10 E-5 Torr	12.9%	19.98
80 mins	340-360 nm	1.45 mg/mL	100C/1 hour	315-320 C	9-10 E-5 Torr	12.8%	19.61
90 mins	380-400 nm	1.45 mg/mL	100C/1 hour	315-320 C	9-10 E-5 Torr	13.1%	18.23

CHAPTER 5: CONCULSIONS

During this study we came to a few realizations early on. The first of these is that we needed add a pre-step layer of lead iodide to have consistent runs. During our runs since we are heating both the lead iodide and the methylammonium iodide at the same time and due to methylammonium iodide being in a gas state it can become deposited on the substrate. While at the same time we are blocking the Lead Iodide from hitting the substrate with a shutter. We found that adding in a pre-step allowed us to have much more consistent results.

Our next realization was that we needed to keep control of the pressure in the chamber. In the beginning it was very difficult to control the MAI pressure, and pump down the system. To allow for us to have more precise control we found that more regular cleaning of the chamber was necessary. This is due to the hydrophilic nature of MAI. Since we didn't have a load lock system for our chamber we would be exposing the MAI coated chamber to moisture every time we opened it up to replace the samples.

We found from the above data that co-evaporated perovskite solar cells are precisely variable sensitive. To have higher efficiency cells we need to have fine control over the MAI pressure, and the overall thickness of the device. Small changes can cause large changes in our current. The control over MAI pressure was the most critical step in making reproducible devices. We needed an almost perfect stoichiometry, this meant that we wanted the specific amount of MAI to react with the PbI2 and this was possible with our method.

REFERENCES

1. Yang, W. S., Noh, J. H., Jeon, N. J., Kim, Y. C., Ryu, S., Seo, J., & Seok, S. I. (2015). High-performance photovoltaic perovskite layers fabricated through intramolecular exchange. Science, 348(6240), 1234-1237. Chicago
2. Lee, M. M., Teuscher, J., Miyasaka, T., Murakami, T. N., & Snaith, H. J. (2012). Efficient hybrid solar cells based on meso-superstructured organometal halide perovskites. Science, 338(6107), 643-647.
3. Snaith, H. J. (2013). Perovskites: the emergence of a new era for low-cost, high-efficiency solar cells. The Journal of Physical Chemistry Letters, 4(21), 3623-3630.
4. Streetman, B. & Banerjee, S. (2006). Solid state electronic devices. Upper Saddle River, N.J: Pearson/Prentice Hall.
5. Honsburg, C., & Bowde, S. (2009, January 1). Quantum Efficiency. Retrieved September 5, 2016, from http://pveducation.org/pvcdrom/quantum-efficiency